

## Comparative evaluation of various drought indices (DIs) to monitor drought status: A case study of Moroccan Lower Sebou basin

Oualid Hakam<sup>1,\*</sup>, Abdennasser Baali<sup>1</sup>, Touria El Kamel<sup>1</sup>, Yousra Ahouach<sup>1</sup>,  
Khalil Azennoud<sup>1</sup>

<sup>1</sup>*Engineering Laboratory of Organometallic, Molecular and Environmental Materials,  
Faculty of Sciences Dhar Mahraz, Sidi Mohamed Ben Abdallah University, Fez, Morocco*

*\*Corresponding author: oualid.hakam@gmail.com*

### Abstract

Due to the lack of studies on drought in the Lower Sebou basin (LSB), the complexity of drought phenomena and the difference in climatic conditions. Therefore, identifying the most appropriate drought indices (DIs) to assess drought conditions has become a priority. Therefore, evaluating the performance of different (DIs) was considered to identify the universal drought indices well adapted to the LSB. Based on data availability, five DIs were used: Standardized Precipitation Index (SPI), Standardized Precipitation and Evapotranspiration Index (SPEI), Reconnaissance Drought Index (RDI), self-calibrated Palmer Drought Severity Index (sc-PDSI) and Streamflow Drought Index (SDI). The DIs were calculated on an annual scale using monthly time series of precipitation, temperature, and river flow from 1984-2016. Thornthwaite's method was used to calculate potential evapotranspiration (PET). In addition, Pearson's correlation ( $r$ ) was analyzed. In addition, data on the yield of durum wheat, soft wheat, and barley for the period 2000-2016 also contributed to the performance evaluation of these indices. The results proved that SPI is suitable for detecting the drought duration and intensity compared to other indices with high correlation coefficients, especially in sub-humid regions, knowing that it tends to give more humid results in stations with semi-arid climates. The multi-scalar indices (SPI, SPEI, and RDI) follow the same trend during the period studied. However, sc-PDSI appears to be the most sensitive to temperature and precipitation by overestimating the drought conditions. In addition, yield/drought correlations tend to be higher for multi-scalar indices than for sc-PDSI. At the same time, slight differences were detected between SPI and SPEI in the performance of agricultural systems. Our results suggest that using multi-scalar indices in drought monitoring and assessment is necessary to have solid conclusions.

**Keywords:** Agricultural system; drought conditions; LSB; Morocco; multi-scalar indices.

### 1. Introduction

Drought is one of the most complex and damaging extreme weather events (Scheff, 2019). It is also considered the least understood of all-natural hazards affecting various environmental systems (Vicente-Serrano *et al.*, 2020). Consequently, there is no universal approach to define, monitor, and quantify its severity and duration (Yihdego *et al.*, 2019) due to its complex spatial-temporal extent and the complex atmospheric and hydrological mechanisms that determine

water availability (Deb *et al.*, 2019). The diversity of drought definitions and the need for long homogeneous climatological series make it difficult to precisely quantify the evolution of these phenomena' frequency and intensity since the beginning of the 20th century (Euzen *et al.*, 2013). Overall, drought is defined as an occurrence caused by below-normal rainfall over an extended period (Swain *et al.*, 2017) and generally precedes other drought categories. As a result, its accurate assessment and prediction provide valuable information to water resource planners and policymakers (Amiri *et al.*, 2018). According to a numerical standard, the drought can be described by its intensity, location, duration, and timing of onset so that drought measurements can be compared across regions and past drought events. For this purpose, various indices and indicators such as meteorological, hydrological, and biophysical parameters have been developed to monitor and assess drought. According to the World Meteorological Organization (WMO & GWP, 2016), drought indices are subdivided into four categories: meteorological, hydrological, agricultural, and socio-economic, each of which could detect different types of drought. Popular meteorological drought indices are numerous and include; Standardized Precipitation Index (SPI; McKee & John, 1993), self-calibrated Palmer Drought Index (sc-PDSI; Wells *et al.*, 2004), Standardized Precipitation and Evapotranspiration Index (SPEI; Vicente-Serrano *et al.*, 2010) and the Reconnaissance Drought Index (RDI; Tsakiris & Vangelis, 2005); while hydrology-related indices include the Surface Water Supply Index (SWSI; Shafer & Dezman, 1982) and Streamflow Drought Index (SDI; Nalbantis & Tsakiris, 2009), and agriculture-related indices include the Crop Moisture Index (CMI; Palmer, 1968) and Soil Moisture Deficit Index (SMDI; Narasimhan & Srinivasan, 2005). Many assessment methods that have been developed over the last century use new technology tools such as remote sensing (RS) and geographic information system (GIS) (Al Jassar & Rao, 2015; Mohammed, 2021), each with its advantages and limitations. They include indices calculated from reflectance via sensors onboard satellites or drones, such as the Normalized Difference Vegetation Index (NDVI; Kogan, 1995) and the Vegetation Condition Index (VCI; Kogan, 1995b). These indices provide a high-resolution measure of vegetation condition and temperature (Bouras *et al.*, 2020) despite the difficulties created during the monsoon seasons (cloud cover). Nevertheless, an index of a drought particular to a given region may not be applied in other areas, given the watersheds' differences in climatic conditions and characteristics (Yang *et al.*, 2017). As a result, many studies have been conducted at different scales worldwide to compare and search for the most appropriate drought index for a given region or basin (Bayissa *et al.*, 2018; Ballah *et al.*, 2021). In Morocco, like the countries of North Africa, drought frequency and severity have been marked during the last decades (Driouech *et al.*, 2021). From a historical point of view, dendrochronological studies have shown that Morocco has experienced over ten centuries (from 1000 to 1984), 146 dry years, or one year in 6 to 7 years (Stockton, 1985). However, few studies have been reported so far (Ed-Daoudi, 2014; Acharki *et al.*, 2019), especially in the Lower Sebou basin (LSB), where the present study is pioneering. Moreover, these earlier studies ignored indices based on evapotranspiration such as RDI, SPEI, and sc-PDSI, knowing that evapotranspiration leads to significant losses of water resources, especially in semi-arid regions. The present study carried out in the Bas Sebou basin (LSB) located in the North-West of Morocco, dominated by the large agrarian plain (Gharb plain) and therefore playing a key role in food security, aims at assessing the agro-meteorological drought by different indices by comparing their performance

during historical droughts and their response in terms of crop yields to identify the most appropriate drought indices for the LSB.

## 2. Materials and methods

### 2.1 Study area

The LSB is located in a climate favorable to agriculture, marked by disturbances that characterize Mediterranean climates. Because it contains meadows and marshes, allowing the installation of fertile and arable land, it can be considered one of Morocco's most prominent agricultural areas. Indeed, the LSB has a sub-humid Mediterranean climate with an oceanic influence, particularly in the western part and semi-arid in the interior (Figure 1. a). Rainfall exceeds 500mm per year in most of the basin, and average temperatures oscillate around 19°C (Table 1). From the point of view of soil cover, the soils in the LSB are diversified, comprising mainly alluvium with clay content ranging from 15% to 55%. These soils are dominated by Tirs, which cover 42% of the area (clayey, allowing slow infiltration of water in depth and favoring the installation of cereal and legume crops), and Dehs (sandy-clay soils) covers 29% of the area. Soils formed by sands occupy 24 % of the area dominated by traditional crops (barley and rye) (Figure 1. c). Therefore, the high rainfall and the importance of the basin's water and biophysical resources, which make it a magnet for large-scale agricultural investments, may lead to a high degree of overexploitation of its resources and consequently make it vulnerable and susceptible to droughts in the future.

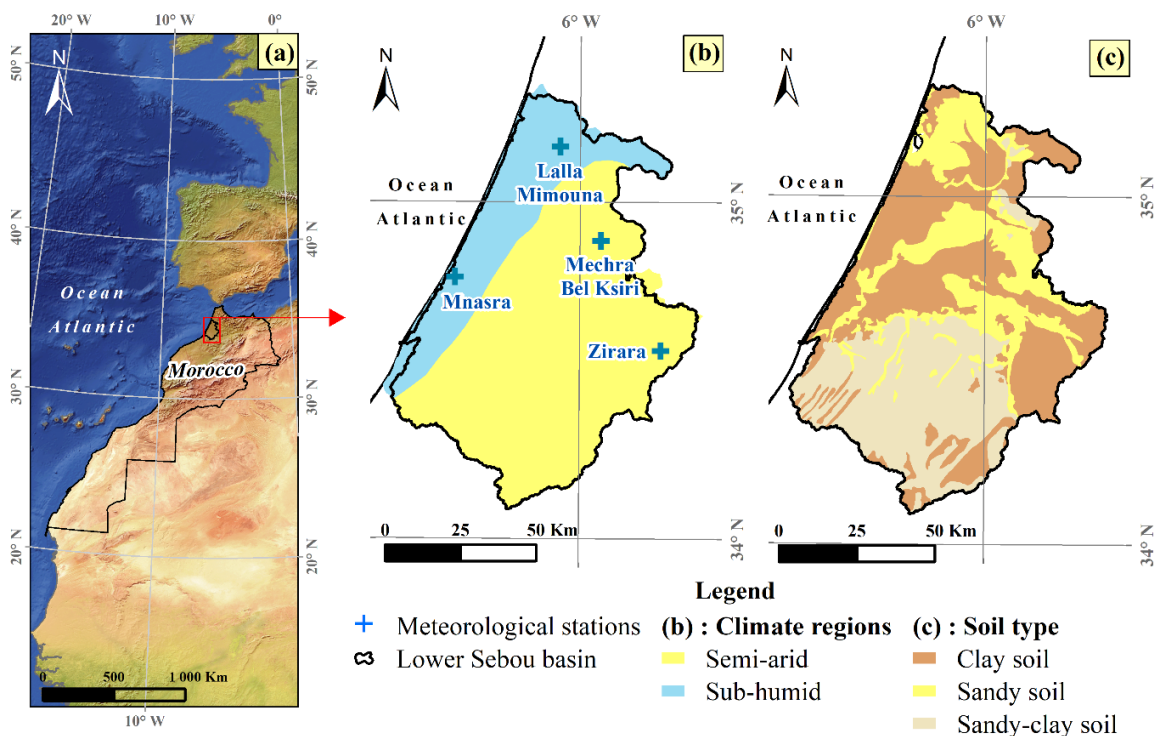


**Fig. 1.** Geographical location of the Lower Sebou basin (LSB) (a); spatial distribution of meteorological stations and climate regions (b); and types of soils (c).

## 2.2 Data and preprocessing

The monthly time series of precipitation, temperatures (4 stations), and stream flows (2 stations) provided by the Sebou Hydraulic Basin Agency (SHBA) for the period 1984-2016 were used and distributed uniformly over the entire LSB (Figure 1). The characteristics of these stations are shown in Table 1. In addition, data on annual production (tonne, t) and harvested area (hectares, ha) of durum wheat, soft wheat, and barley were acquired from the statistical services of the Ministry of Agriculture. As a result, the time series of rainfed cereal yields in tonne per hectare (t.ha<sup>-1</sup>) represent the ratio between annual production (t) and harvested area (ha) during the period 2000-2016 for each province of the LSB (Sidi Kacem and Kenitra).

**Table 1.** Characteristics of synoptic stations in the LSB and average annual precipitation, potential evapotranspiration (PET), and climatic conditions.

Stations	Station type	Rainfall (mm/year)	PET (mm/year)	Climate condition	Geographical coordinates		
					Lng (°W)	Lat (°N)	Z (m)
Lalla Mimouna	Meteorological, gauge	574,7	1157,5	Sub humid	6.11	34.85	15
Mechra Bel Ksiri	Meteorological, gauge	515	1441,4	Semi-arid	5.96	34.57	24
Mnasra	Meteorological	567	1239,5	Sub humid	6.48	34.46	10
Zirara	Meteorological	387	1480	Semi-arid	5.74	34.24	55

**Note:** PET: Potential evapotranspiration calculated based on the Thornthwaite equation; Lng: longitude; Lat: latitude; Z: altitude in meters.

## 2.3 Selection of drought indices (DIs)

Drought assessment requires different approaches: a perception/observation-based approach, an approach based on remote sensing data, a model-based approach, and an approach based on in-situ data (hydro-meteorological/climatic). This set of approaches is generally always accompanied by several indicators and indices essential to assess and monitor the different types of drought and the aspect of the hydrological cycle. More than 150 applied drought indices (DIs) and indicators worldwide. About 40 are commonly used to monitor spatial and temporal variability in drought-prone regions (WMO & GWP, 2016). However, in the absence of a universal definition for drought, no single index can meet the objectives of this study under different global climates.

In general, in situ data approach offers direct and simple methods for monitoring the onset, spread, and intensity of droughts (Senay *et al.*, 2015). According to national and international studies on the robustness and weakness of drought indices (Ezzine *et al.*, 2014; WMO & GWP, 2016), the indices used are the Standardized Precipitation Index (SPI), the Standardized Precipitation Evapotranspiration Index (SPEI), the Reconnaissance Drought Index (RDI) and

the self-calibrating Palmer Drought Severity Index (sc-PDSI). It should also be pointed out that the RDI, SPEI, and sc-PDSI are being used for the first time in the LSB and that the Streamflow Drought Index (SDI) is selected as the hydrological drought index.

#### 2.4 Calculation of drought indices (DIs)

The DIs chosen are characterized by their specificity and complexity of calculation. Except for SPI, they integrate different water balance components based only on cumulative precipitation. Their calculation could be performed on time scales of 1, 3, 6, 9, and 12 months, except for sc-PDSI, which has a flexible but almost annual timescale (Zhong *et al.*, 2020). From this defect, sc-PDSI cannot identify both shorter and longer droughts (Vicente-Serrano *et al.*, 2010). In addition, many studies have shown that multi-scalar DIs such as SPI, SPEI, and RDI correlate well with sc-PDSI on a time scale of around 12 months (Vicente-Serrano *et al.*, 2015; MAF & GDWM, 2018). Hence, the study focused on the variation in drought characteristics over a longer time scale (12 months), as reflected by sc-PDSI, SPI-12, SPEI-12, and RDI-12.

For the normalization of DIs, a two-parameter gamma distribution for SPI and RDI and a three-parameter log-logistic distribution for SPEI were chosen (Table 2). For greater precision, the calculation of SPEI (Equation 2) and sc-PDSI require the estimation method of potential evapotranspiration (PET), while that of RDI does not depend on it (Vangelis *et al.*, 2013). The use of the Thornthwaite method in the case of SPEI and sc-PDSI is recommended in several works (Dai, 2011).

**Table 2.** Fitting variables and probability distribution were selected for SPI, SPEI, RDI, and SDI.

Drought index	Variables	Chosen probability distribution
1. Standardized Precipitation Index (SPI)	P	Gamma
2. Standardized Precipitation Evapotranspiration Index (SPEI)	P, T	Log-Logistic (3 parameters)
3. Reconnaissance Drought Index (RDI)	P, T	Gamma
4. self-calibrating Palmer Drought Severity Index (sc-PDSI)	P, T, AWC	(-)
5. Streamflow Drought Index (SDI)	Streamflow	Log-normal

**Note:** T: monthly mean air temperature; P: monthly accumulated rainfall; AWC: available water capacity.

Standardized Precipitation Index (SPI): This index is based on historical rainfall records at a given location (McKee *et al.*, 1993) to calculate the probability of rainfall at any time scale between 1 and 48 months. This study uses the SPI Generator application available at the National Drought Mitigation Center maintained by the University of Nebraska to calculate SPI values. Negative and positive values indicate dry and wet conditions, respectively. The drought intensity category ranges from greater than 2.0 (Extremely wet) to less than -2.0 (Extremely dry) (Table 3).

$$SPI = \frac{P_i - P_m}{S} \quad (1)$$

With  $P_i$ : the rain of month or year  $i$ ;  $P_m$ : the average rain of the series;  $S$ : the standard deviation of the series on the considered time scale. A gamma distribution was used to overcome the constraint of rainfall that is not normally distributed during the year.

Standardized Precipitation Evapotranspiration Index (SPEI): is an index that was developed by Vicente-Serrano et al., (2010) at the Pirenaico Institute of Ecology in Zaragoza (Spain); this relatively recent index is based on the monthly difference between rainfall and potential evapotranspiration (PET) calculated according to the Thornthwaite's method (Thornthwaite, 1948). It also uses the same drought category as SPI (Table 3), and its calculation requires the R package "SPEI" (Beguería & Vicente-Serrano, 2009).

The difference between cumulative monthly rainfall and evapotranspiration is calculated as follows:

$$D_i = P_i - PET_i \quad (2)$$

$D_i$  values are aggregated at different time scales, following the same procedure as for SPI. The annual drought levels for each SPEI range are given in Table 3.

Reconnaissance Drought Index (RDI): This index is the result of work undertaken by Tsakiris & Vangelis (2005) at the National Technical University of Athens (Greece); it contains both a simplified water balance equation that takes into account rainfall and potential evapotranspiration (PET). Its product is estimated by three values: the initial value, the standardized value, and the normalized value. The normalized value is similar to the SPI and can be directly compared to it over several periods of 1, 3, 6, 9, 12, or more months.

The initial value of the index for a given period, indicated by the number of months ( $k$ ) in a year, is calculated using the following equation:

$$DI = \frac{\sum^{j=k} P_i}{\sum PET_i} \quad (3)$$

$P_i$  and  $PET_i$  are the monthly precipitation and potential evapotranspiration of a hydrologic year that generally begins in October (Morocco). RDI values follow the log-normal or gamma distribution. This ratio is normalized similarly to the equations used to normalize the SPI to obtain the RDI values.

Streamflow Drought Index (SDI): The calculations of this index established by Nalbanties & Tsakiris (2009) are made using the monthly values of streamflow and the normalization methods used for the SPI to produce a drought index according to streamflow. RDI and SDI were calculated using software named *DrinC* (Tigkas *et al.*, 2015), developed by the Water Resources Rehabilitation and Management Laboratory of the National Technical University of Athens.

It has been suggested that a time series of monthly discharge volumes  $Q_{i,j}$  denotes the hydrologic year and  $j$  the month of the hydrologic year ( $j=1$  for October and  $j=12$  for September) based on this series.

$$V_{i,k} = \sum_{j=1}^{3k} Q_{i,j} \quad i = 1,2, \dots \quad k = 1,2,3,4 \quad (4)$$

Where  $V_{i,k}$  is the cumulative volume of discharge for the  $i^{\text{th}}$  hydrologic year and the  $k^{\text{th}}$  reference period.

SDI index is defined for each reference period  $k$  of the  $i^{\text{th}}$  hydrological year as follows:

$$SDI_{i,k} = \frac{V_{i,k} - \bar{V}_k}{S_k} \quad (5)$$

Where  $\bar{V}_k$  and  $S_k$  are, respectively, the average and the standard deviation of cumulative discharge volumes of the reference period ( $k$ ), SDI values, and severity designations are similar to SPI, RDI, and SPEI (Table 3).

Self-calibrating Palmer Drought Severity Index (sc-PDSI): Initially, the proposed Palmer Drought Severity Index (PDSI) was a drought index based on semi-physical data (Palmer, 1965). It integrates the soil water balance from a simple soil moisture model. Afterward, the PDSI algorithm was modified by Wells et al. (2004) in the self-calibrated Palmer Drought Severity Index (sc-PDSI). This index could automatically adjust the empirical constants in the PDSI calculation with dynamically calculated values. The computational function of sc-PDSI is based on C++ source codes developed by the Risk Management Agency (AGR) and the University of Nebraska as part of the Greenleaf project (<http://greenleaf.unl.edu>). More detailed algorithms and calculation procedures are available (Wells *et al.*, 2004).

The sc-PDSI index is calculated from the time series of monthly rainfall and temperature and fixed parameters related to soil or surface characteristics at each location. The sc-PDSI values are divided into nine categories ranging from -4 (dry) to 4 (wet), using a comprehensive classification based on the severity of dry or wet conditions (Table 3).

**Table 3.** Wet/Dry classification of DI<sub>s</sub>.

Class	SPI, SPEI, DRI and SDI Value	Class	sc-PDSI value
Extremely Wet (E. W)	$\geq 2$	Extremely Wet (E. W)	$\geq 4$
Severe Wet (S. W)	1.5 to 1.99	Severe Wet (S. W)	3 to 3,99
Moderately Wet (M. W)	1.0 to 1.49	Moderately Wet (Mo. W)	2 to 2,99
Normal (N)	0.99 to -0.99	Mild Wet (Mi. W)	1 to 1,99
Moderately Dry (Mo. D)	-1 to -1.49	Incipient Wet (I. W)	0,5 to 0,99
Severely dry (S. D)	-1.5 to -1.99	Normal (N)	0,49 to -0,49
Extremely Dry (E. D)	$\leq -2$	Incipient Dry (I. D)	-0,50 to -0,99
		Mild Dry (MiD)	-1 to -1,99
		Moderately Dry (M. D)	-2 to -2,99
		Severely dry (S. D)	-3 to -3,99
		Extremely Dry (E. D)	$\leq -4$

## 2.5 Evaluation of drought indices (DIs)

Given the vast number of DIs developed and the efforts of scientific committees, it is also essential to consider the practical application as each index has its own limits, calculates drought differently, and compares several indices using the same regional data. To assess the performance of DIs used, statistical relationships were first calculated to provide useful diagnostics in the performance assessment. Consequently, the analyses were carried out as follows: **(i)** time series analysis to assess the Spatio-temporal distribution of meteorological drought; **(ii)** Pearson (R) correlation analysis between SPI-12, SPEI-12, RDI-12, and sc-PDSI; **(iii)** comparison of identified drought characteristics and **(iv)** comparison of DIs during major historical drought episodes. Knowing that drought is one of the significant abiotic stresses affecting grain yield and quality (Pervez *et al.*, 2017), the last step **(v)** is focused on the performance of the various drought indices (DIs) in assessing the impact of climate on crops, using rainfed cereal yield data, to reflect the capabilities of each index in monitoring agricultural drought. Pearson (R) correlation analysis was also used to examine the relationship between drought indices and crop yields. In the analysis, anomalies in grain yield were calculated by removing the linear trend from the crop yield time series to exclude non-climatic factors. Variations in crop yields usually depend on several factors in addition to climatic ones, such as new management technologies and innovative practices. Therefore, the detrended yield was calculated using the Z-score method to exclude the bias due to non-climatic factors. (Bouras *et al.*, 2020).

## 3. Results and discussion

### 3.1 Spatiotemporal distribution of drought episodes

Four DIs were calculated to evaluate the Spatio-temporal distribution of meteorological drought at each station of LSB. The results obtained showed different intensities and episodes of the drought sequences, even during the same year and the same period of time. Then, Pearson correlation coefficients (R) were derived from time series values of DIs for all stations. Each station is associated with all other stations, forming a 4 x 4 correlation coefficient matrix.

#### 3.1.1 Spatiotemporal distribution of SPI

The SPI-12 values across the stations show a single drought intensity with uniform drought episodes (Figure 2). At Lalla Mimouna station, 2016 was the driest year with extreme drought episodes. Episodes of drought during 1995, 2005, and 2016 at the various stations were observed. 2005 and 2016 were marked by severe to extreme droughts in Lalla Mimouna station, while Mnasra station recorded relatively low intensities, even though the two stations are located in the coastal zone. In the case of the stations located inside the LSB, Zirara station experienced episodes of extreme drought in 1995, while Mechra Bel Ksiri station experienced a severe drought in 2016. In general, all stations have shown SPI-12 values indicating identical drought years with a strong correlation between them ( $0.76 \leq r \leq 0.92$ ) due to the high homogeneity of precipitation in the LSB and the dominance of the oceanic climate influenced by local topography.



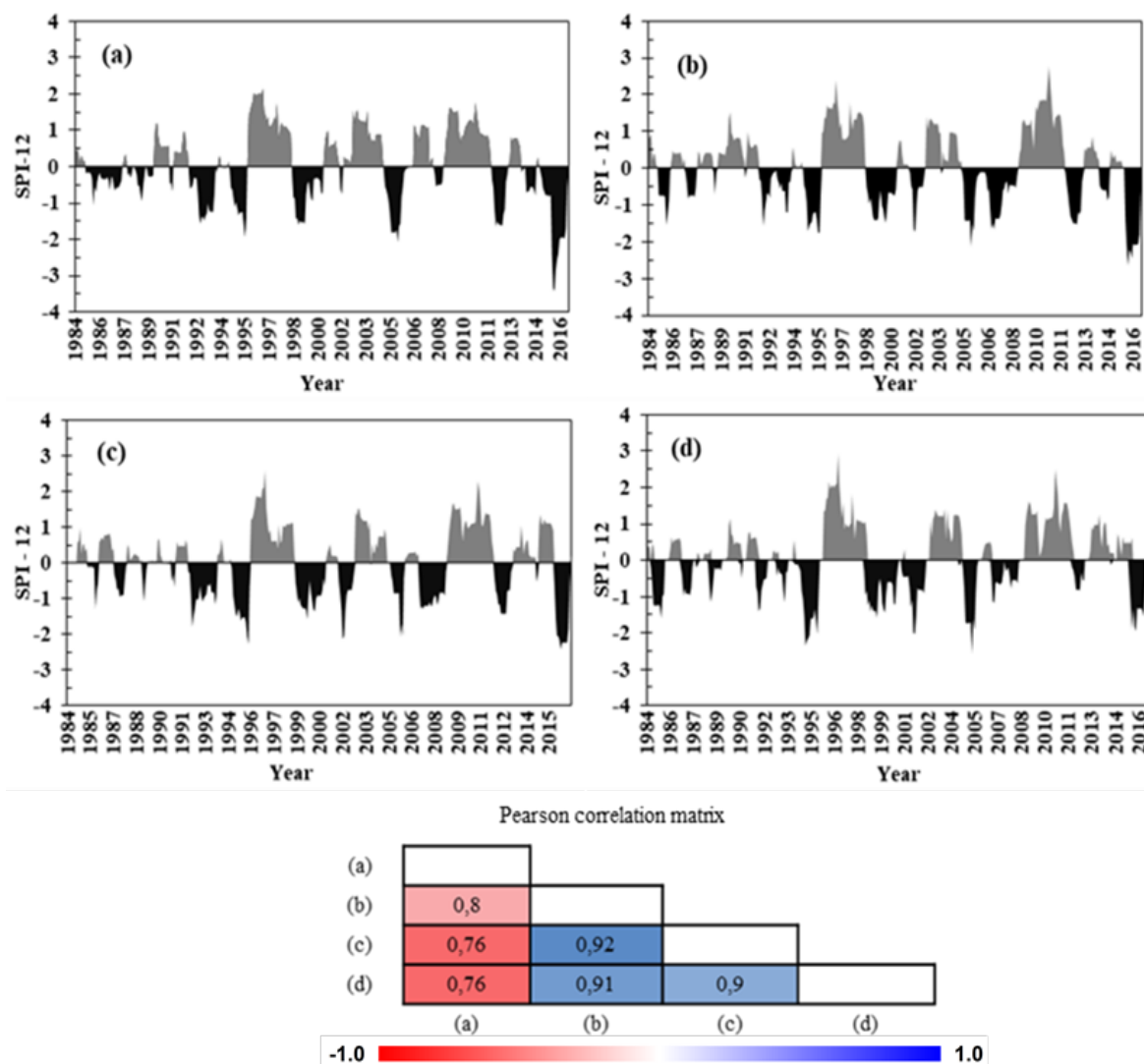


**Fig. 2.** Spatiotemporal distribution of SPI-12 in the LSB and correlation matrix of SPI-12 between the different stations: (a) Lalla Mimouna, (b) Mechra Bel Ksiri, (c) Mnasra, (d) Zirrara.

### 3.1.2 Spatiotemporal distribution of SPEI

Figure 3 shows that the Spatio-temporal distribution of SPEI-12 values reflects a very distinct heterogeneity, reflected by a very weak correlation between the Lalla Mimouna station and Mnasra station ( $r = 0.48$ ). The majority of SPEI-12's values show that the LSB has experienced extreme to severe droughts, especially during 2006 and 2016, given that 2016 was the driest year in 33 years, marked by the influence of a strong El Niño (WMO, 2017). SPEI-12 shows the prevalence of extreme droughts in 1995, 2006, and 2016 at Mechra Bel Ksiri station, followed by severe droughts at Mnasra station, and moderate droughts are very frequent at Zirara station. However, Lalla Mimouna station has experienced severe to extreme droughts during the last decade and longer duration. Regarding the recorded wet years, Lalla Mimouna and Zirara stations recorded frequent wet years, while the other stations are marked by a single extremely wet period between 2009 and 2011.

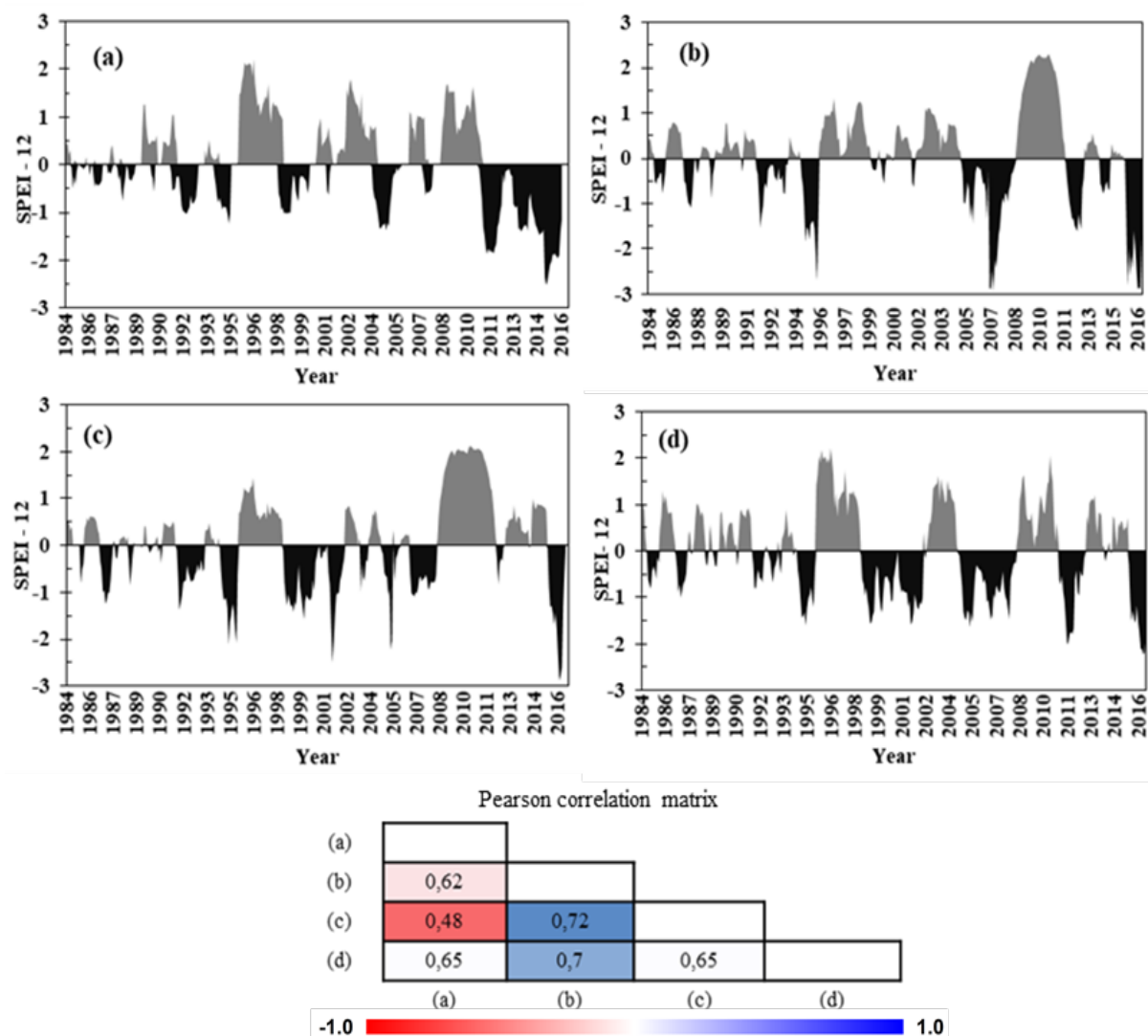


**Fig. 3.** Spatiotemporal distribution of SPEI-12 in the LSB and correlation matrix of SPEI-12 between the different stations: (a) Lalla Mimouna, (b) Mechra Bel Ksiri, (c) Mnasra, (d) Zirrara.

### 3.1.3 Spatiotemporal distribution of RDI

The spatiotemporal variation of RDI-12 in the LSB (Figure 4) shows that the year 2016 had the maximum severity (-3.44), indicating an extreme drought followed by the year 2005 (-2.76). Mechra Bel Ksiri station had only one extremely wet and long period between 2009 and 2011. RDI-12 values show an abundance of moderate droughts at Mechra Bel Ksiri station, except for a single extreme drought in 2016. Mnasra and Zirara stations have comparatively more dry years than the other stations, especially Mechra Bel Ksiri station, where the magnitude of drought is more important during the last years. Figure 4 also shows generalized droughts produced during 1995, 2006, and 2016. However, the events occurred during apparently random years with low correlation coefficients ( $0.62 \leq r \leq 0.87$ ) compared to SPI-12.

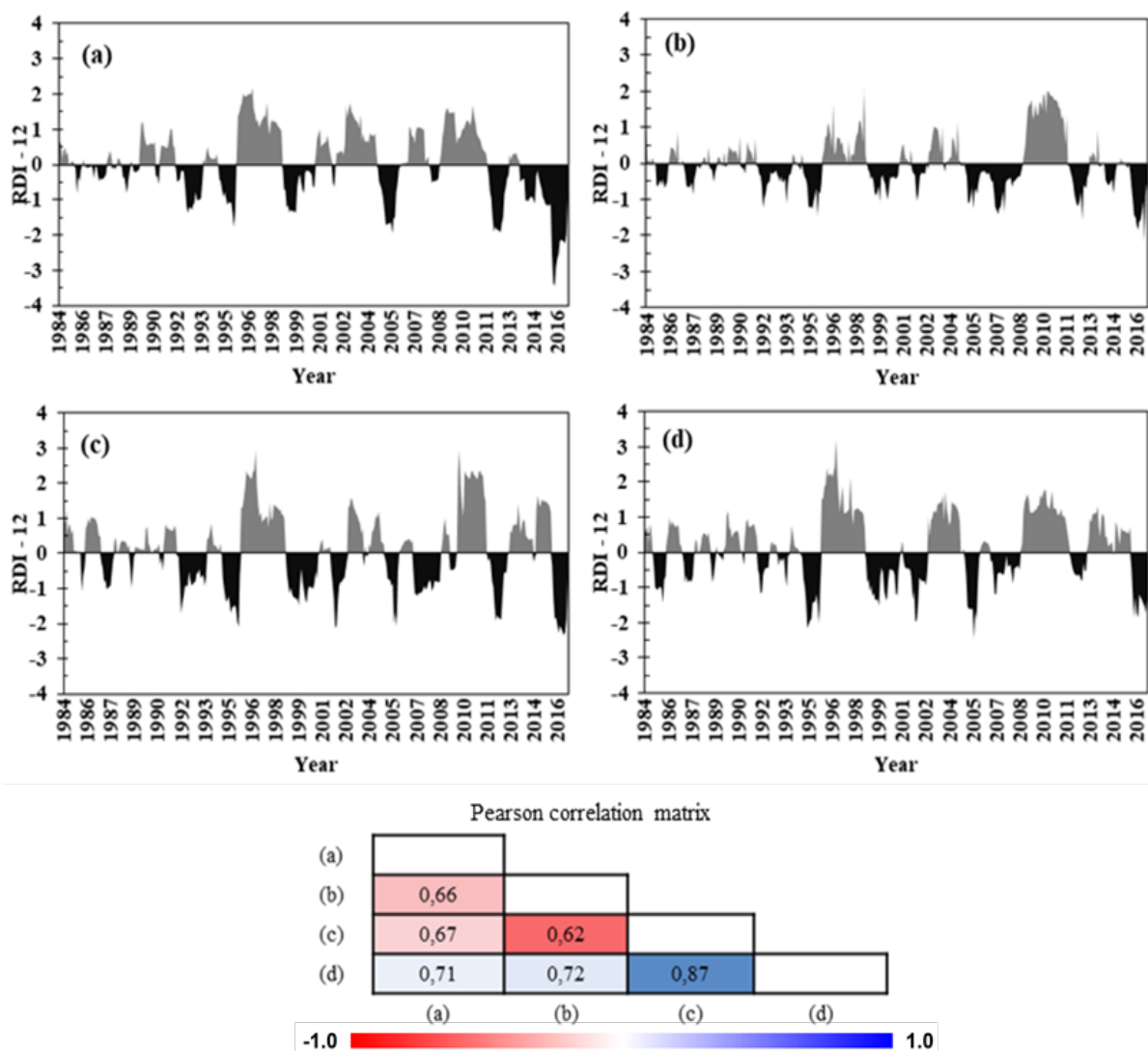


**Fig. 4.** Spatiotemporal distribution of RDI-12 in the LSB and correlation matrix of RDI-12 between the different stations: (a) Lalla Mimouna, (b) Mechra Bel Ksiri, (c) Mnasra, (d) Zirrara.

### 3.1.4 Spatiotemporal distribution of sc-PDSI

Unlike the other indices the abundance of drought episodes is well marked in all stations with very wide severities (Figure 5), probably due to algorithms incorporating more biophysical factors to calculate sc-PDSI (Abrantes *et al.*, 2021). In addition, the evolution of sc-PDSI during the period 1984-2016 revealed new episodes of drought, sometimes of long duration, particularly in the periods 1985-1988, 1992-1995, 1998-2002, 2005-2008, and 2012-2016. It is also interesting to note that the Lalla Mimouna station showed relative humidity even during the periods of drought recorded by the other stations. However, since 2012, the rainfall has been reduced, and ETP has increased due to increased temperature. Thus, the severity and duration of induced drought overestimated by sc-PDSI results in station-to-station variation in drought episodes' intensity, severity, and duration. These episodes are almost similar in the stations except Lalla Mimouna station, which showed relatively weakest correlation coefficients, compared to the other stations ( $0.42 \leq r \leq 0.45$ ). This difference could be explained by the

difference in latitudinal position between the Lalla Mimouna station and the other stations on the one hand. On the other hand, the presence of dense forests maintains the water retention capacity of the soils (Xing *et al.*, 2018). The highest correlation ( $r = 0.79$ ) is recorded between the two stations (Mechra Bel Ksiri and Zirara), which are on the inland side of the basin (degree of continentality).

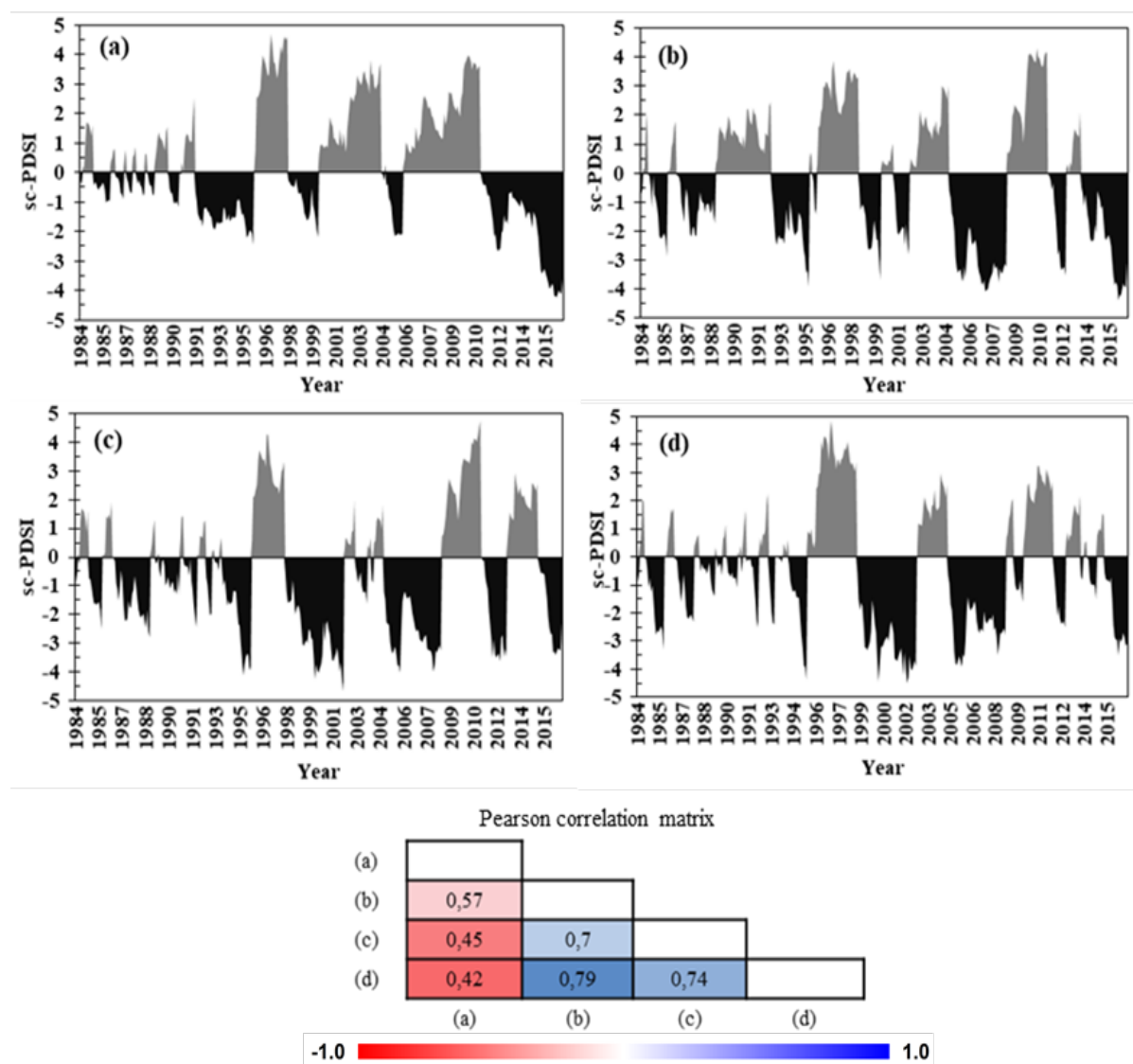


**Fig. 5.** Spatiotemporal distribution of sc-PDSI-12 in the LSB and correlation matrix of sc-PDSI-12 between the different stations: (a) Lalla Mimouna, (b) Mechra Bel Ksiri, (c) Mnasra, (d) Zirara.

### 3.2 Correlation between different drought indices (DIs)

The Pearson correlation's values ( $R$ ) were obtained by comparing the outputs of the different stations and taken as references for discussion. Figure 6 clearly illustrates the importance of SPI-12 and RDI-12 indices in the different stations of the LSB, where the results obtained show a generally similar behavior (Figure 1, 4). This similarity of outputs between SPI and RDI indices is not unique in this region (Merabti *et al.*, 2018; Pathak & Dodamani, 2019), and their correlation coefficients coupled with other indices are comparatively higher ( $0.77 \leq r \leq 0.99$ )

(Figure 6). However, in the Mechra Bel Ksiri station, SPI-12 reacted relatively better with other indices compared to RDI-12. This difference is justified because RDI-12 recorded fewer dry years at this station than SPI-12, SPEI-12, and sc-PDSI (Figure 4). According to the World Meteorological Organization (WMO), SPI-12 remains the most recommended index for drought monitoring. The results obtained from the correlations showed that SPI-12, which requires rainfall data, can effectively replace RDI-12, SPEI-12, and sc-PDSI because it is positively correlated with high correlation coefficients up to  $r = 0.99$  and statistically significant (Figure 6). In most stations, SPI-12 correlates well with SPEI-12 except at station Zirara ( $r = 0.84$ ) due to the fact that SPI-12 and SPEI-12 work better in humid areas than in arid regions or semi-arid ones (Yang *et al.*, 2017). However, there is minimal correlation between SPI-12 and sc-PDSI. SPI-12 captures anomalies in the rainfall pattern, while the water balance-based indices (sc-PDSI, SPEI-12, and RDI-12) estimate anomalies in the climatic water balance. More specifically, strong consistency is noted between the multi-scalar indices (SPI, RDI, and SPEI) compared to sc-PDSI. Low correlations were manifested between SPEI-12, RDI-12, and sc-PDSI compared to SPI-12 in Mechra Bel Ksiri and Zirara stations, knowing that the strongest correlations were mentioned in the Lalla Mimouna station (Figure 6). These results confirm the abundance of drought indicated by SPEI-12 and sc-PDSI in the Zirara station due to the semi-arid climate (Figure 3, 5), which is why SPI cannot monitor and assess the drought in such a context (Nikbakht & Hadeli, 2021). However, the inclusion of temperature in the algorithm of SPEI and sc-PDSI, in particular, does not provide sufficient information for the Lalla Mimouna station, where temperatures are relatively stationary series. It was also found that SPI has little difference with sc-PDSI and SPEI when time trends in temperature are evident (Vicente-Serrano *et al.*, 2010). Overall, the Spatio-temporal evolution of DI<sub>s</sub> in the LSB generally follows a similar change pattern consistent with the results in other regions (Jain *et al.*, 2015; Adnan *et al.*, 2018).

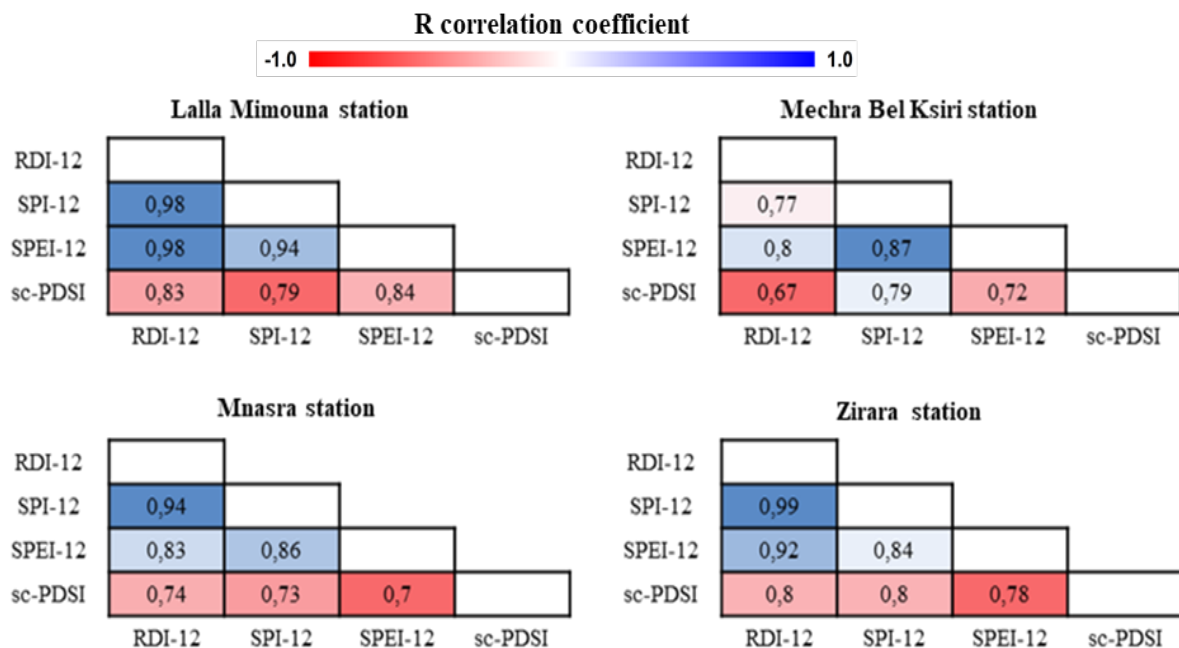


**Fig. 6.** Pearson correlation matrix of DI<sub>s</sub> for all stations of LSB.

### 3.3 Assessment of the characteristics of meteorological drought

Considering the duration and severity of drought identified during 1984-2016, categories of dry months were determined (Table 3, Figure 7), which allowed us to visualize their relative frequencies in each station (Figure 8). Knowing that the relative frequency indicates the percentage of each drought severity class according to the index considered.

The  $DI_s$  used, except sc-PDSI, where the number of dry months is relatively high, showed an identical number of dry months in all stations (Figure 7). Zirara station received more dry months than the other stations, especially Lalla Mimouna station. It should be noted that RDI-12 shows identical and highest relative frequencies, in particular in the class of moderate droughts (Mo. D), reaching (97%) at Mechra Bel Ksir station and 92% at Zirara station (Figure 8). RDI is more suitable for the characterization of drought in semi-arid regions (Moghimi *et al.*, 2020). However, the sc-PDSI index shows relative frequencies of dry months in all categories and all stations. In addition, according to the indices used, the moderate drought class is the most dominant in all the stations. Consequently, and based on the results obtained above, Lalla Mimouna station remains the least subject to drought episodes in connection with its situation in latitude, which frequently undergoes the passage of cyclonic depressions towards the North without taking into account its proximity to the coast, knowing that the Mnasra station despite its coastal location, it recorded drought episodes almost similar to the Zirara station (Figure 7) (El Jihad *et al.*, 2014).

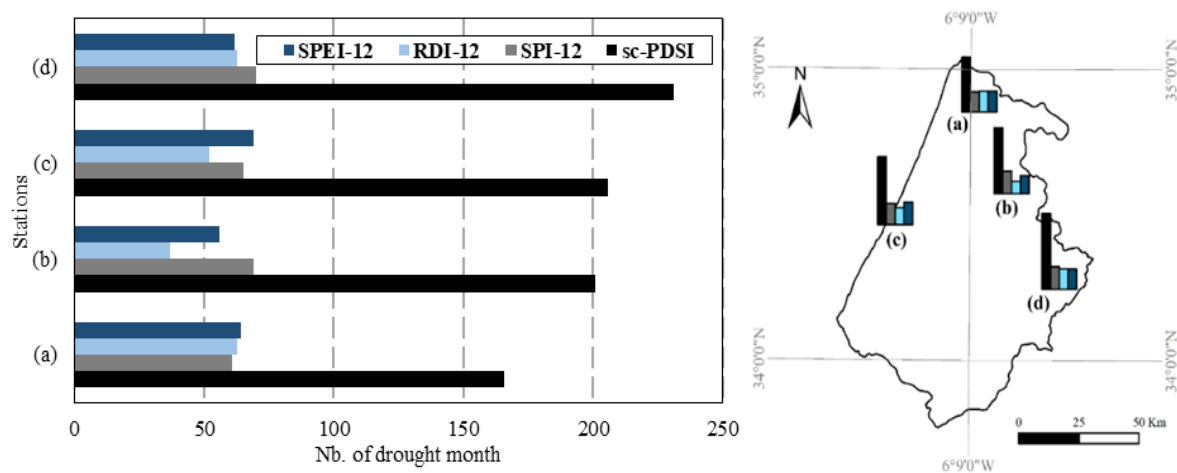


**Fig. 7.** Spatial distribution of the number of dry months of stations in LSB: (a) Lalla Mimouna, (b) Mechra Bel Ksiri, (c) Mnasra, (d) Zirara, for the period 1984-2016.

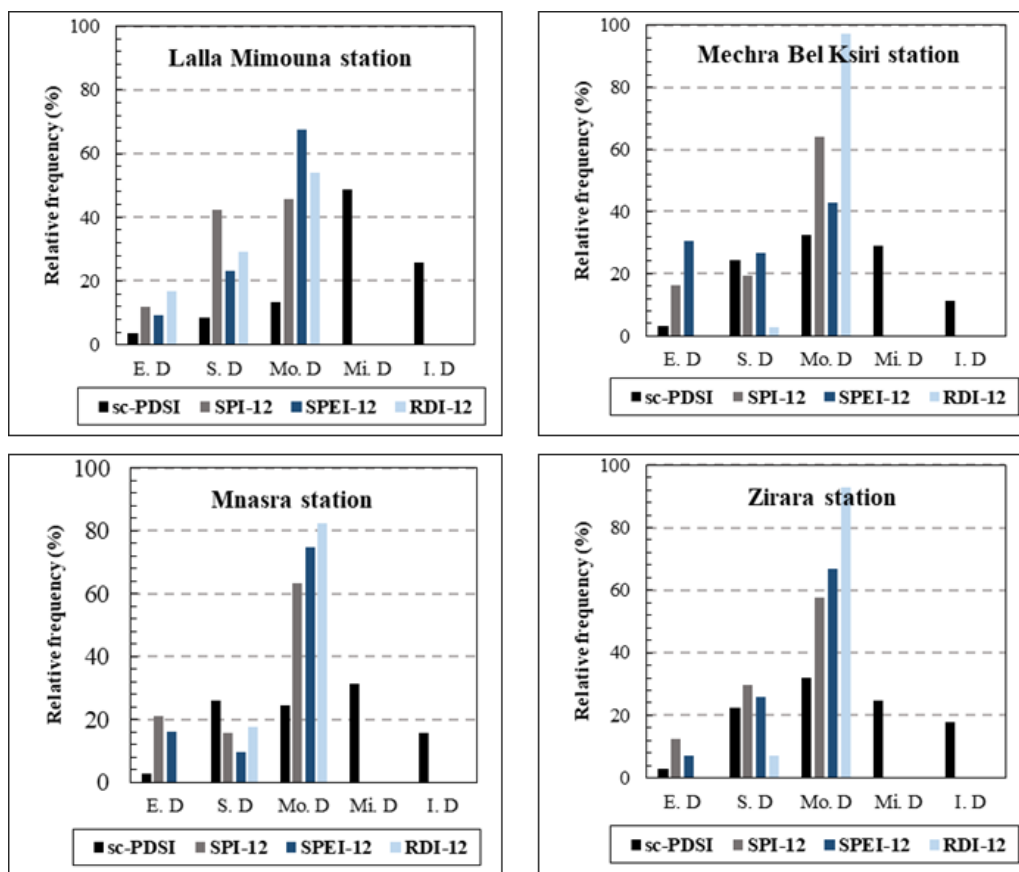


**Fig. 8.** Histograms of relative frequency of drought classes; ('Extreme Dry (ED)', 'Severe Dry (SD)', 'Moderate Dry (Mo.D)', 'Mild drought (Mi.D)' and 'Incipient drought (ID)'.) According to the four indices for the period 1984-2016.

**Note:** The drought classes (Mild drought (Mi. D) and incipient drought (I. D)) have been assigned for sc-PDSI.

### 3.4 Performance of drought indices (DI<sub>s</sub>)

The performance of DI<sub>s</sub> in the LSB practically requires the search for a period when the drought is well defined and recognized. To achieve this, three approaches were implemented, including the above results, the calculation of the drought index based on streamflow (SDI), and the climate archives.

According to the High Commission for Planning report, the LSB experienced a severe drought that lasted from 1991 to 1995, the year of which 1995 was declared to be catastrophic from an agricultural point of view (Laouina, 2006). This situation is also reflected in surface water (dams and rivers), accompanied by a deficit of 75% of the average flow of the entire Sebou watershed (Bzioui, 2004). In terms of the fluvial flow of the LSB, the chronological series of the stream flows of the main rivers used to determine SDI-12 have also determined and approved the presence in the two gauging stations of a severe to extreme hydrological drought (Mechra Bel Ksiri and Lalla Mimouna stations) (Figure 9). In addition, all DI<sub>s</sub> also showed severe to extreme drought situations for the same period, 1991-1995 (Figure 2, 3, 4, 5).

To assess the performance of  $DI_s$  during historical droughts, time series of indices and indicators such as temperatures (T) and rainfall (P) from the period 1991-1995 are compared with those of average monthly temperatures and precipitation for the period 1984-2016. This operation allowed us to establish the adequacy of each meteorological drought index in determining the onset, end, and severity of drought. In all stations, the monthly values of temperatures and precipitations (1991-1995) and the values of the  $DI_s$  clearly showed that the deficit of monthly precipitations is lower than the average (Figure 10). SPI-12, SPEI-12, and RDI-12 have the same trend and a good correlation (Figure 6), particularly at the Lalla Mimouna station (January 1991 until September 1992), despite the significant precipitation and evapotranspiration showing the effect of precipitation anomalies on evapotranspiration. Therefore, SPEI-12 and RDI-12 work similarly to SPI-12, which includes rainfall. The similarity between SPI-12, RDI-12, and SPEI-12 shows that rainfall is the primary determinant of meteorological drought in the north of LSB. SPEI-12/RDI-12 at Lalla Mimouna station and from October 1992 onwards respond to drought less than SPI-12, which marks moderate to severe droughts. This is due to the calculation of SPI-12 based on precipitation that could indicate drier situations in sub-humid regions (Lalla Mimouna station) or wetter in the semi-arid areas (Zirara station from May 1992 to July 1993). On the other hand, Pathak & Dodamani (2019) showed that the SPI, RDI, and SPEI indices follow a similar overall behavior in the semi-arid regions. Figure 10 also shows a very high similarity between SPI-12/RDI-12, especially at the Zirara station, where they have the highest correlation coefficient ( $r = 0.99$ ) (Figure 6). The RDI and SPI indices are most appropriate for the characterization of drought in arid and semi-arid regions (Xu *et al.*, 2015). The evolution of sc-PDSI differs from station to station in showing a relatively exaggerated trend during dry and even wet periods, given that this index takes into account biophysical factors that are dependent on location factors of the station, unlike other indices which are focused on rainfall and ETP. Through in-depth observation of the relationship between indicators (T, P) and meteorological  $DI_s$ , sc-PDSI appears to be most sensitive to temperatures and precipitation by overestimating drought conditions (Jiang *et al.*, 2015). It experienced a sharp decline in value after the rainfall deficit in November 1991 at Lalla Mimouna, Mnasra, and Zirara stations. It should also be noted that the rainfall deficit was not significant from November 1991 to October and that SPI-12, SPEI-12, and RDI-12 indices indicated this period as usual to wet, unlike sc-PDSI, which maintained its negative values (Figure 10). Similarly, during wet episodes, the sc-PDSI curve shows upward trends in November 1995 at Lalla Mimouna and Mnasra stations and in June 1995 at Mechra Bel Ksiri and Zirara stations (Figure 10). Knowing that the sc-PDSI considers the soil's water retention capacity, which was high during this period, especially in forested areas. The values indicated by sc-PDSI are the most negative during this year, except for the stations Zirara and Mechra Bel Ksiri. The month of June recorded significant rainfall of storm origin, which increased the value of sc-PDSI (Figure 10). Thornthwaite's method overestimates the impact of temperature on evapotranspiration calculation (Trenberth *et al.*, 2007; Hobbins *et al.*, 2008), as evidenced by decreased sc-PDSI values. Penman Monteith's equation was not used given the lack of data on its parameters and the strong correlation and similarity between this method and the Thornthwaite method globally.



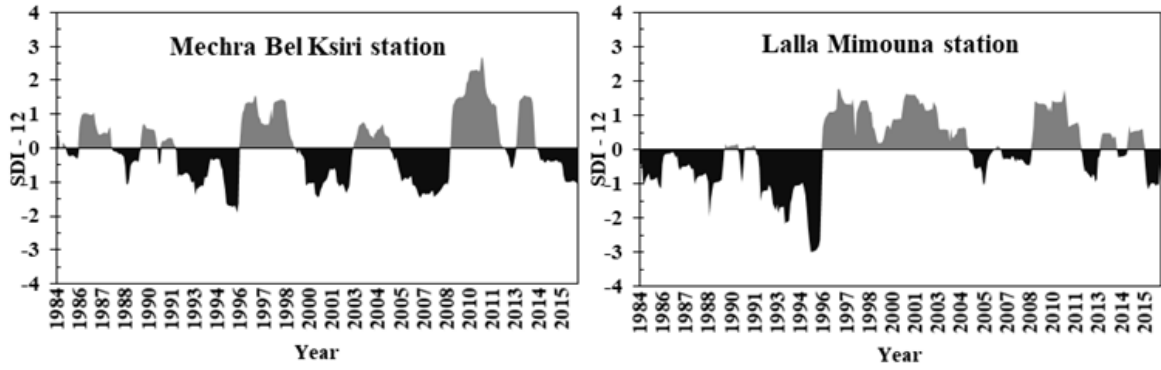


Fig. 9. Annual change in SDI during the period 1984-2016.

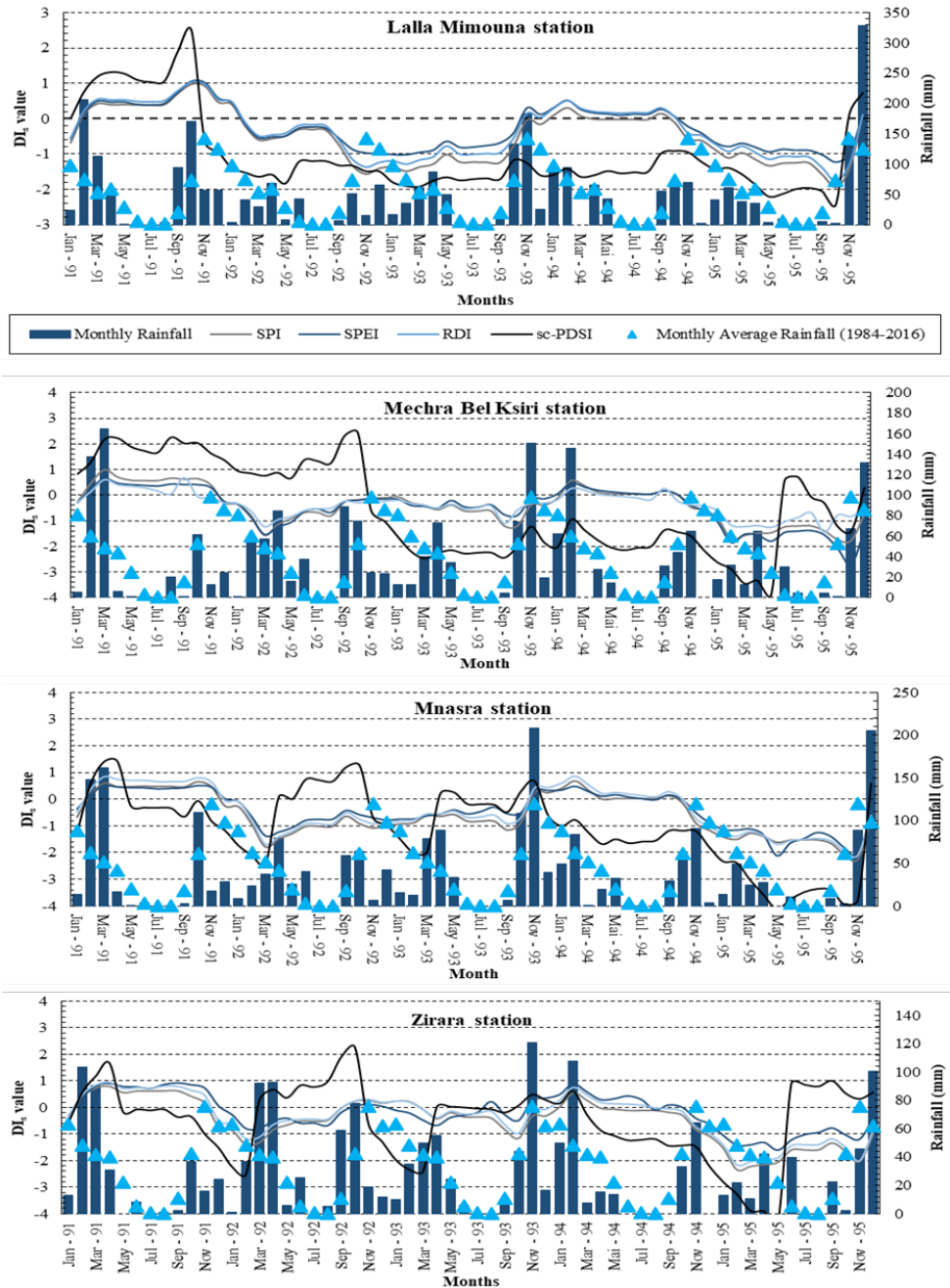
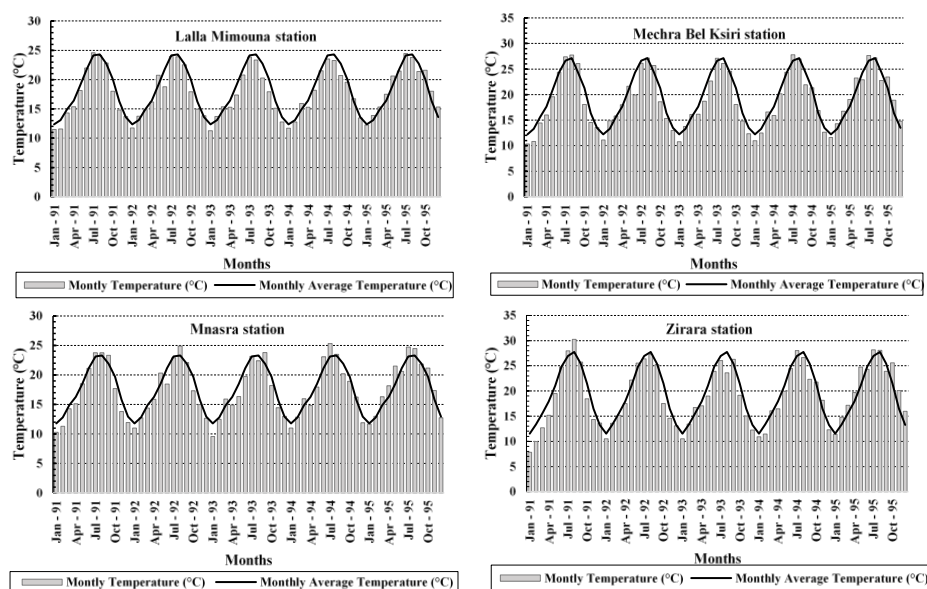


Fig. 10. Time series of 5-year  $DI_s$ , monthly rainfall, and average rainfall for 1984-2016 at LSB stations.



**Fig. 11.** Monthly temperatures for the period 1991-1995 and monthly averages temperatures for the period 1984-2016 at LSB stations.

### 3.5 Temporal responses of drought indices (DI<sub>s</sub>) to crop yields

The applied drought indices (DI<sub>s</sub>) were evaluated to determine their satisfaction with the good index criterion and their usefulness in the LSB. The correlation analysis between the detrended crop yield and the (DI<sub>s</sub>) was also carried out for the four weather stations for 16 years. It should be noted that the RDI, SPI, and SPEI graphs were recovered by the maximum correlation coefficient of 1 to 12 months. Similar to the previous results and independent of the cereal type and time scale considered, our results showed that the multi-scalar DI<sub>s</sub> (RDI, SPI, and SPEI) have a greater ability to reflect the impacts of drought on rainfed cereal yields compared to sc-PDSI, especially at the beginning of the growing season (October to December) (Figure 12, 13, 14). This is mainly due to their flexibility to reflect the negative impacts of climate on different regions with very other characteristics (Vicente-Serrano et al., 2011). This difference is essential in agro-meteorology, as crops do not react in the same way to water deficit. This is consistent with previous similar studies in various regions that reported that these indices were effective in monitoring the impacts of drought on agriculture (Mahmoudi *et al.*, 2019; Peña-Gallardo *et al.*, 2019; Wable *et al.*, 2019).

However, the sc-PDSI performance evaluation results showed some exceptions during the intermediate and final growth stages, which is consistent with the critical growth stages of cereals according to the phenological calendar and may be helpful for monitoring purposes. This evaluation also found significant differences in the influence of drought conditions on barley, durum, and soft wheat yields in different months. During the early to mid-growing season, the correlation coefficients (R) obtained from the multi-scalar indices are mainly around 0.6 from October to April and around 0.4 in May before decreasing to about 0.3 in June (close to harvest). This is due to the growing cycle of cereals that usually ends in June and the low moisture demand, which underlines the importance of adequate moisture conditions during the winter season for the excellent development and growth of cereals. Minor differences between

the multi-scalar DIs suggest that SPEI is the best performer for all cereal crops, although the SPI was lower in relation to barley yields (Figure 12). Durum and soft wheat yields (Figure 13, 14) show stronger correlations than barley yields, especially for SPI, which depends only on the amount of rainfall in the calculation (Figure 12). This is due to the physiological characteristics of barley and the sandy texture of the soil, being less dependent on water availability at the germination and grain filling stage compared to wheat (Mamnouie *et al.*, 2006) and less prone to water stress under drought conditions due to their higher transpiration coefficient (Fischer *et al.*, 1998). Moreover, the results indicate a similarity between the temporal response of barley, durum and soft wheat to drought conditions, although, in Morocco, barley is generally grown later than wheat and in soils with low water holding capacity. They also indicated that the temperature factor is more important than precipitation in monitoring and assessing agricultural drought, indicating that extreme changes in mean temperature during the most sensitive growth stages can negatively affect rainfed cereal crops. Furthermore, the results of the comparative assessment in the previous sections suggest the role of rainfall in monitoring and assessing meteorological drought in the LSB. The superiority of SPI suggests that the simplicity and availability of data give a well-defined power. In addition, the use of precipitation and evapotranspiration (water balance) in the calculation of SPEI constitutes, thanks to its better correlation between drought and cereal yields, the most adequate solution to address the characterization of agricultural drought in Morocco to have the necessary information to set up an insurance product, offering a guarantee on cereal production in rainfed areas and against drought risks.

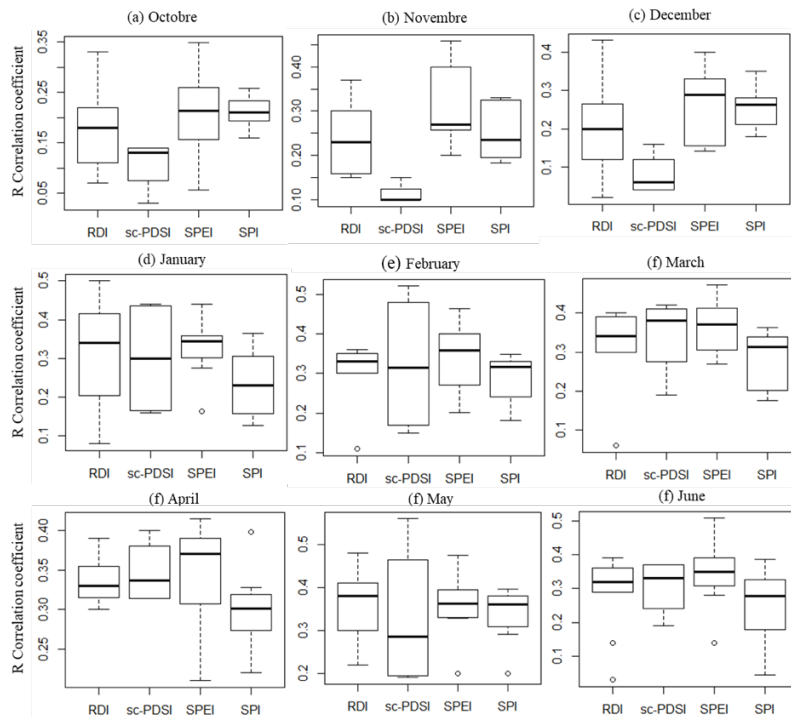


**Fig. 12.** Correlation coefficients (R) between DIs and detrended rainfed cereal yield during the barley-growing season (October of the previous year to June of the current year). The upper and lower limits of the box indicate the upper and lower quartiles, respectively. The line in the box indicates the median, the lines outside the box indicate the upper and lower bounds, and the circles show the outlier in the data set.

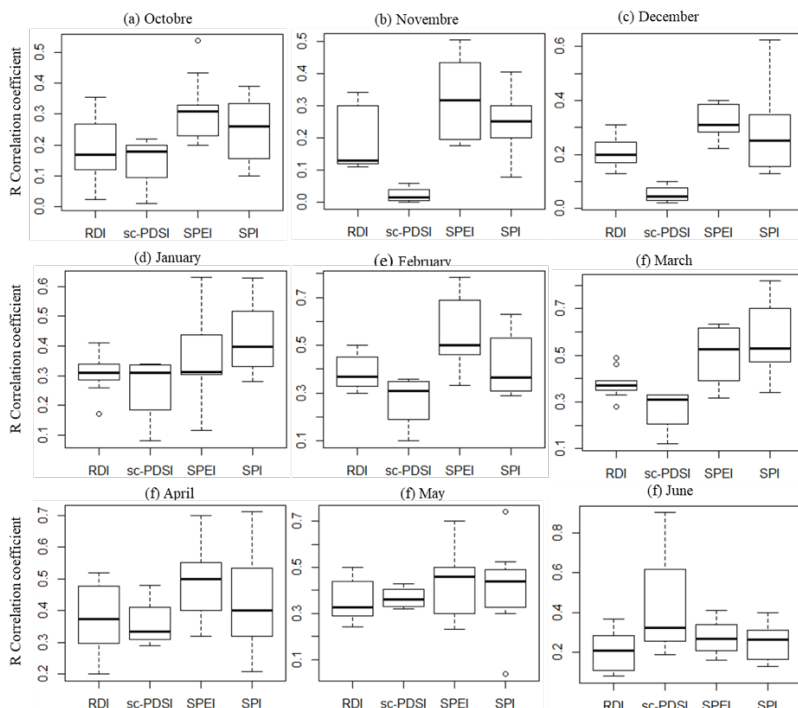


**Fig. 13.** Correlation coefficients (R) between DIs and detrended rainfed cereal yield during the durum wheat-growing season (October of the previous year to June of the current year). The upper and lower limits of the box indicate the upper and lower quartiles, respectively. The line in the box indicates the median, the lines outside the box indicate the upper and lower bounds, and the circles show the outlier in the data set.

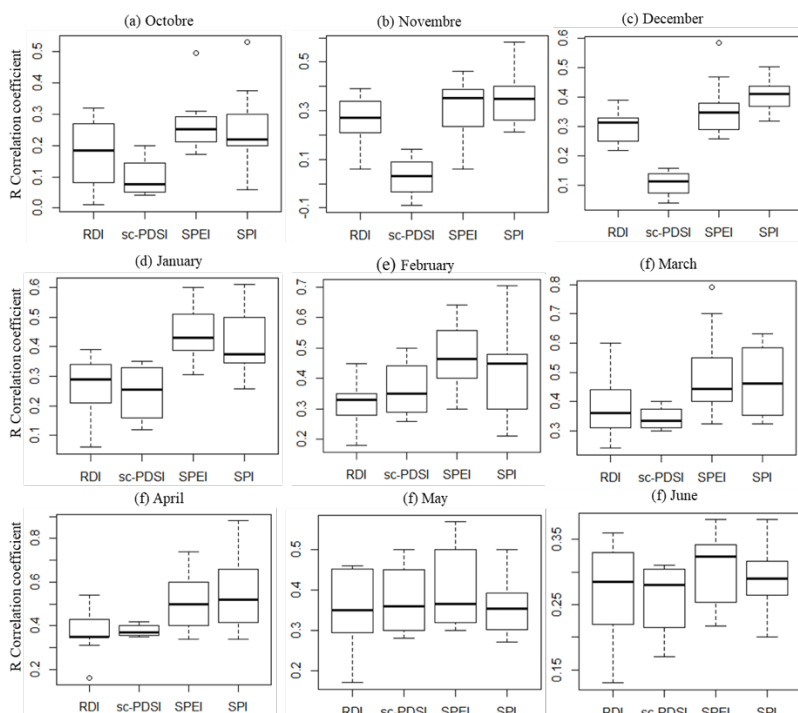


**Fig. 14.** Correlation coefficients (R) between DIs and detrended rainfed cereal yield during the soft wheat-growing season (October of the previous year to June of the current year). The upper and lower limits of the box indicate the upper and lower quartiles, respectively. The line in the box indicates the median, the lines outside the box indicate the upper and lower bounds, and the circles indicate the outlier in the data set.

#### 4. Conclusions

The study carried out in the LSB assessed the regional applicability and performance of four drought indices (DIs), SPI, SPEI, RDI, and sc-PDSI, based on time series of precipitation and temperature at four meteorological stations during the period 1984-2016 and of cereal yield (2000-2016). The Spatio-temporal distribution of drought episodes using drought indices (DIs) shows that the severity and intensity of droughts have increased since 2012. All the multi-scalar indices reveal four typical annual droughts in 1995, 1999, 2012, and 2016. The exception is the sc-PDSI index, which has shown new drought episodes with a sometimes long-lasting trend. More importantly, the evaluation of the performance of the drought indices for monitoring the effect of climate on cereal yields showed the best performance of the multi-scalar indices, while small differences were detected between the SPI and the SPEI/RDI in the performance of farming systems. Barley and wheat yields are more vulnerable to drought during the intermediate growth stage (spring), and moisture conditions in winter also have an impact on crop yields.

Climatic and agricultural conditions in the Lower Sebou Basin are very diverse. This highlights the need to establish accurate and effective indices to assess and monitor the effect of climate, particularly in vulnerable agricultural areas. Furthermore, climate variation leads to yield losses due to water deficits. Therefore, the authors suggest that further analysis should be carried out using more sophisticated satellite indicators to elucidate further the climatic and biophysical mechanisms responsible for the Spatio-temporal distribution of agricultural drought in the LSB.

#### ACKNOWLEDGMENTS

The authors thank the Dhar El Mahraz Faculty of Sciences for its financial and logistical support. The authors also wish to thank the development team of the free and open-source geographic information system (QGIS), the R language packages to perform statistical processing, and the Sebou Hydraulic Basin Agency (SHBA) for providing meteorological data for the study area. Finally, we also thank the invaluable suggestion of the anonymous reviewers.

#### References

- Abrantes, A. C., Serejo, J., & Vieira-Pinto, M. (2021)** The Association between Palmer Drought Severity Index Data and Tuberculosis-like Lesions Occurrence in Mediterranean Hunted Wild Boars. *Animals*, 11(7) : 2060.
- Acharki, S., Amharref, M., El Halimi, R., & Bernoussi, A. S. (2019)** Évaluation par approche statistique de l'impact des changements climatiques sur les ressources en eau: application au périmètre du Gharb (Maroc). *Revue des Sciences de l'Eau/Journal of Water Science*, 32(3): 291-315.
- Adnan, S., Ullah, K., Shuanglin, L., Gao, S., Khan, A. H., & Mahmood, R. (2018)** Comparison of various drought indices to monitor drought status in Pakistan. *Climate Dynamics*, 51(5-6), 1885-1899.

**Al Jassar, H.K., & Rao, K. S. (2015)** Assessment of soil moisture through field measurements and AMSR-E remote sensing data analysis over Kuwait desert. *Kuwait Journal of Science*, 42(2).

**Amiri, M.A., Conoscenti, C., & Mesgari, M.S. (2018)** Improving the accuracy of rainfall prediction using a regionalization approach and neural networks. *Kuwait Journal of Science*, 45(4).

**Ballah, A., & Benaabidate, L. (2021)** Assessing the performance of various meteorological drought indices in capturing historic droughts in the south of Algeria. *Arabian Journal of Geosciences*, 14(13): 1-11.

**Bayissa, Y., Maskey, S., Tadesse, T., Van Andel, S.J., Moges, S., Van Griensven, A., & Solomatine, D. (2018)** Comparison of the performance of six drought indices in characterizing historic drought for the upper Blue Nile basin, Ethiopia. *Geosciences*, 8(3): 81.

**Beguiría, S., & Vicente-Serrano, S. (2009)** DIGITAL.CSIC. Récupéré sur SPEI Calculator.

**Stockton, C. (1985)**. Current research progress toward understanding drought. *Proceedings, Drought, Water Management and Food Production*, 21-35.

**Bouras, E., Jarlan, L., Er-Raki, S., Albergel, C., Richard, B., Balaghi, R., & Khabba, S. (2020)** Linkages between rainfed cereal production and agricultural drought through remote sensing indices and a land data assimilation system: a case study in Morocco. *Remote Sensing*, 12(24).

**Bzioui, M. (2004)** Rapport national 2004 sur les ressources en eau au Maroc. UN Water-Africa, 94.

**Dai, A. (2011)** Characteristics and trends in various forms of the Palmer Drought Severity Index during 1900–2008. *Journal of Geophysical Research: Atmospheres*, 116.

**Deb, P., Kiem, A.S., & Willgoose, G. (2019)** A linked surface water-groundwater modeling approach to more realistically simulate rainfall-runoff non-stationarity in semi-arid regions. *Journal of Hydrology*, 575: 273-291.

**Driouech, F., Stafi, H., Khouakhi, A., Moutia, S., Badi, W., ElRhaz, K., & Chehbouni, A. (2021)** Recent observed country-wide climate trends in Morocco. *International Journal of Climatology*, 41.

**Ed-Daoudi, S. (2014)** Evolutions et changements des extrêmes pluviométriques au niveau de la zone Souss-Massa-Draa (Maroc) : L'aspect sécheresse. Sciences and technologies Faculty, Marrakesh, Morocco.

**Euzen, A., Eymard, L., & Gaill, F. (2013)** Le développement durable à découvert. CNRS Éditions, Paris.

**Ezzine, H., Bouziane, A., & Ouazar, D. (2014)** Seasonal comparisons of meteorological and agricultural drought indices in Morocco using open short time-series data. *International Journal of Applied Earth Observation and Geoinformation*, 26:36-48.

- Fischer, R.A., Rees, D., Sayre, K. D., Lu, Z.M., Condon, A.G., & Saavedra, A.L. (1998)** Wheat yield progress associated with higher stomatal conductance and photosynthetic rate, and cooler canopies. *Crop Science*, 38(6): 1467-1475.
- Hobbins, M.T., Dai, A., Roderick, M.L., & Farquhar, G.D. (2008)** Revisiting the parameterization of potential evaporation as a driver of long-term water balance trends. *Geophysical Research Letters*, 35 (12).
- Jain, V.K., Pandey, R.P., Jain, M.K., & Byun, H.R. (2015)** Comparison drought indices for appraisal of drought characteristics in the Ken River Basin. *Weather Clim Extremes* 8: 1–11.
- Kogan, F.N. (1995)** Droughts of the late 1980s in the United States as derived from NOAA polar-orbiting satellite data. *Bulletin of the American Meteorology Society*, 76(5): 655–668.
- Laouina, A. (2006)** Gestion durable des ressources naturelles et de la biodiversité au Maroc. *Prospectives, Maroc*.
- Mahmoudi, P., Rigi, A., & Kamak, M.M. (2019)** A comparative study of precipitation-based drought indices with the aim of selecting the best index for drought monitoring in Iran. *Theoretical and Applied Climatology*, 137(3): 3123-3138.
- Mamnouie, E., Fotouhi Ghazvini, R., Esfahani, M., & Nakhoda, B. (2006)** The effects of water deficit on crop yield and the physiological characteristics of barley (*Hordeum vulgare* L.) varieties. *Journal of Agricultural Science and Technology*, 8(3): 211-219.
- McKee, T.B., Doesken, N.J., & Kleist, J. (1993)** The relationship of drought frequency and duration to time scales. In *Proceedings of the 8th Conference on Applied Climatology* 17:179-183.
- Merabti, A., Meddi, M., Martins, D.S., & Pereira, L.S. (2018)** Comparing SPI and RDI applied at local scale as influenced by climate. *Water resources management*, 32(3): 1071-1085.
- Ministry of Agriculture and Forestry (MAF), & General Directorate of Water Management (GDWM). (2018)** Antalya basin drought management plan, Turkey.
- Moghimi, M.M., Zarei, A.R., & Mahmoudi, M.R. (2020)** Seasonal drought forecasting in arid regions, using different time series models and RDI index. *Journal of Water and Climate Change*, 11(3): 633-654.
- Mohammed, D.A. (2021)** Integrated remote sensing and GIS techniques to delineate groundwater potential area of Chamchamal basin, Sulaymaniyah, NE Iraq. *Kuwait Journal of Science*, 48(3).
- Nalbantis, I., & Tsakiris, G. (2009)** Assessment of hydrological drought revisited. *Water Resources Management*, 23(5): 881-897.
- Narasimhan, B. and R. Srinivasan (2005)** Development and evaluation of Soil Moisture Deficit Index (SMDI) and Evapotranspiration Deficit Index (ETDI) for agricultural drought monitoring. *Agricultural and Forest Meteorology*, 133(1): 69–88.

- Nikbakht, J., & Hadeli, F. (2021)** Comparison of SPI, RDI and SPEI indices for drought monitoring under climate change conditions (Case study: Kermanshah station). *Journal of Agricultural Meteorology*, 9(1): 14-25.
- Palmer, W.C. (1968)** Keeping track of crop moisture conditions, nationwide: the new Crop Moisture Index. *Weatherwise*, 21: 156–161.
- Pathak, A.A., & Dodamani, B.M. (2019)** Comparison of meteorological drought indices for different climatic regions of an Indian river basin. *Asia-Pacific Journal of Atmospheric Sciences*, 1-14.
- Peña-Gallardo, M., Vicente-Serrano, S.M., Domínguez-Castro, F., & Beguería, S. (2019)** The impact of drought on the productivity of two rainfed crops in Spain. *Natural Hazards and Earth System Sciences*, 19(6): 1215-1234.
- Pervez, K., Ullah, F., Mehmood, S., & Khattak, A. (2017)** Effect of *Moringa oleifera* Lam. leaf aqueous extract on growth attributes and cell wall-bound phenolics accumulation in maize (*Zea mays* L.) under drought stress. *Kuwait Journal of Science*, 44(4).
- Scheff, J. (2019)** A unified wetting and drying theory. *Nature Climate Change*, 9(1): 9-10.
- Senay, G.B., Velpuri, N.M., Bohms, S., Budde, M., Young, C., Rowland, J., & Verdin, J.P. (2015)** Drought monitoring and assessment: remote sensing and modeling approaches for the famine early warning systems network. In *Hydro-meteorological hazards, risks and disasters*, 233-262.
- Shafer, B.A. & L.E. Dezman, (1982)** Development of a Surface Water Supply Index (SWSI) to Assess the Severity of Drought Conditions in Snowpack Runoff Areas. *Proceedings of the Western Snow Conference*, Colorado State University, Fort Collins, United States.
- Swain, S., Patel, P., & Nandi, S. (2017)** Application of SPI, EDI and PNPI using MSWEP precipitation data over Marathwada, India. In *2017 IEEE International geoscience and remote sensing symposium (IGARSS)*.
- Thornthwaite, C.W. (1948)** Una aproximación para una clasificación racional del clima. *Geographical Review*, 38: 85-94.
- Tigkas, D., Vangelis, H., & Tsakiris, G. (2015)** DrinC: a software for drought analysis based on drought indices. *Earth Science Informatics*, 8(3): 697-709.
- Trenberth, K.E., Jones, P.D., Ambenje, P., Bojariu, R., Easterling, D., Klein Tank, A., ... & Soden, B. (2007)** Observations: surface and atmospheric climate change. Chapter 3. *Climate change*, 235-336.
- Tsakiris, G., & Vangelis, H.J.E.W. (2005)** Establishing a drought index incorporating evapotranspiration. *European water*, 9(10): 3-11.
- Vangelis, H., Tigkas, D., & Tsakiris, G. (2013)** The effect of PET method on Reconnaissance Drought Index (RDI) calculation. *Journal of Arid Environments*, 88: 130-140.



**Vicente-Serrano, S.M., Beguería, S., & López-Moreno, J.I. (2010)** A multiscalar drought index sensitive to global warming: the standardized precipitation evapotranspiration index. *Journal of Climate*, 23(7): 1696-1718.

**Vicente-Serrano, S. M., Quiring, S. M., Pena-Gallardo, M., Yuan, S., & Dominguez-Castro, F. (2020)** A review of environmental droughts: Increased risk under global warming?. *Earth-Science Reviews*, 201.

**Vicente-Serrano, S.M., Van der Schrier, G., Beguería, S., Azorin-Molina, C., & Lopez-Moreno, J.I. (2015)** Contribution of precipitation and reference evapotranspiration to drought indices under different climates. *Journal of Hydrology*, 526: 42-54.

**Wable, P. S., Jha, M. K., & Shekhar, A. (2019)** Comparison of drought indices in a semi-arid river basin of India. *Water resources management*, 33(1): 75-102.

**Wells, N., Goddard, S., & Hayes, M.J. (2004)** A self-calibrating Palmer drought severity index. *Journal of Climate*, 17(12): 2335-2351.

**World Meteorological Organization (2017)** WMO Statement on the State of the Global Climate in 2016.

**World Meteorological Organization (WMO) and Global Water Partnership (GWP) (2016)** Handbook of Drought Indicators and Indices (M. Svoboda and B.A. Fuchs). Integrated Drought Management Programme (IDMP), Integrated Drought Management Tools and Guidelines Series 2. Geneva, Switzerland.

**Xing, Z., Yan, D., Wang, D., Liu, S., & Dong, G. (2018)** Experimental analysis of the effect of forest litter cover on surface soil water dynamics under continuous rainless condition in North China. *Kuwait Journal of Science*, 45(2).

**Xu, K., Yang, D., Yang, H., Li, Z., Qin, Y., & Shen, Y. (2015)** Spatio-temporal variation of drought in China during 1961–2012: A climatic perspective. *Journal of Hydrology*, 526: 253-264.

**Yang, Q., Li, M., Zheng, Z., & Ma, Z. (2017)** Regional applicability of seven meteorological drought indices in China. *Science China Earth Sciences*, 60(4): 745-760.

**Yihdego, Y., Vaheddoost, B., & Al-Weshah, R.A. (2019)** Drought indices and indicators revisited. *Arabian Journal of Geosciences*, 12(3): 69.

**Zhong, L., Hua, L., & Yan, Z. (2020)** Datasets of meteorological drought events and risks for the developing countries in Eurasia. *Big Earth Data*, 1-33.

**Submitted:** 26/04/2021

**Revised:** 08/08/2021

**Accepted:** 11/09/2021

**DOI:** 10.48129/kjs.13911